

Repeated Impact-Driven Plume Formation On Enceladus Over Megayear Timescales

AMIR SIRAJ¹ AND ABRAHAM LOEB¹

¹*Department of Astronomy, Harvard University, 60 Garden Street, Cambridge, MA 02138, USA*

ABSTRACT

Water plumes erupting from the ‘tiger stripe’ features on the south pole of Enceladus are thought to connect to a global subsurface ocean. Proposed origins for the initial stress necessary to form the ‘tiger stripes’ include a giant impact, which would require true polar wander, or tensile stresses, which would require a partial freezing of the subsurface ocean. A further issue with these hypotheses is that the ‘tiger stripes’ may be short-lived. We show here that impact resurfacing can seal off plumes and mass loss can lead to their compression and closure over ~ 1 Myr. Since plumes are observed at present, a mechanism by which new plumes can be generated every ~ 1 Myr and by which such plumes are most likely to form at the south pole is needed. We propose and investigate the possibility that impacts constitute a adequate repeating source for the continual instigation of fractures and plumes. We find that the rate of impacts on Enceladus suggests the formation of $\sim 10^3$ independent plume systems per Gyr, the vast majority on the south pole, and is consistent with the Cassini-derived age of the south pole for a lunar-like bombardment history, our estimates of fracture lifetimes, and with the needed parameters for parallel fracture propagation. The model favors a bombardment history similar to that of Triton over one more similar to that of the Galilean satellites, and favors a cumulative power-law index of 4.2 for impactors with radius, $1 \text{ km} < R < 10 \text{ km}$.

Keywords: planets and satellites: surfaces – planets and satellites: physical evolution – planets and satellites: oceans – meteorites, meteors, meteoroids – minor planets, asteroids: general

1. INTRODUCTION

Enceladus’ physical libration suggests the existence of a global subsurface ocean (Hurford et al. 2009; Thomas et al. 2016). The South Pole Terrain (SPT) of Enceladus contains unique ‘tiger stripe’ features emitting plumes of water, thought to be fractures in the moon’s icy shell connecting to a subsurface ocean (Patthoff & Kattenhorn 2011; Porco et al. 2014; Ingersoll & Nakajima 2016; Kite & Rubin 2016; Le Gall et al. 2017; Hemingway & Mittal 2019). The plumes have made Enceladus a target for astrobiological research and a candidate in the search for a second genesis (Hsu et al. 2015; Postberg et al. 2017; Waite et al. 2017; Benner 2017; Judge 2017; McKay et al. 2018; Klenner et al. 2020; Glein & Waite 2020; Taubner et al. 2020).

The cratering of the SPT indicates a young age relative to the rest of the surface of Enceladus, ~ 1 Myr for a lunar-like impact chronology (Porco et al. 2006).

A weakness of the impact hypothesis is the requirement of true polar wander to explain the location of the SPT (Tajeddine et al. 2017; Nimmo & Pappalardo 2006; Roberts & Stickle 2017). The Hemingway et al. (2019) model presents a plausible formation scenario for the tiger stripes as a result of ridge loading and bending stresses after one of the central fractures is initiated, however the tensile stresses (Manga & Wang 2007; Rudolph & Manga 2009) necessary to initiate the first fracture would require a few hundred meters of ocean freezing (Hemingway et al. 2019). While it is not clear whether the thermal history of Enceladus would support such a freezing (Craft et al. 2011; Czechowski 2014; Travis & Schubert 2015), this *Letter* presents two arguments for why plumes may be short-lived, one based on mass loss, and the other due to impact resurfacing, and thus by the Copernican principle, there should be a time-independent and repeatable origin for plumes.

A repeatable source for an initial fracture giving rise to plumes is cratering by heliocentric debris. In this *Letter*, we explore the cratering rate and the implication for the rate at which plumes on different parts of Enceladus could be formed. We also show that plumes likely have

limited lifetimes due to resurfacing caused directly by cratering from smaller objects as well as compression of the icy shell due to mass loss.

Our discussion is structured as follows. In Section 2, we explore the mechanism for fracture formation from impactors and evaluate the predicted rates of fracture for different pole thicknesses of ice on Enceladus. In Section 3 we discuss the lifetime of fractures, which is limited by compression due to global mass loss and by the rate of impact resurfacing. Finally, in Section 4, we summarize key predictions of our model.

2. IMPACT FRACTURING

2.1. Fracture formation

An icy impactor with mass M , radius R , and speed v penetrates an icy shell with thickness L to a depth, $\sim 4R/3$, where it has roughly encountered an equal volume of material over approximately the crossing time of that distance, $\sim 4R/3v$. The impactor releases a large part of the lost kinetic energy as a pressure wave that emanates from the submerged surface and propagates throughout the icy shell, decaying as $(x/R)^{-1.8}$, where x is the distance from the impactor's surface (Shirai et al. 2008). The pressure at the bottom of the icy shell is,

$$P_d \sim \frac{3Mv^2}{8\pi R^{1.2}L^{1.8}}. \quad (1)$$

Adopting the dynamic shear strength of water ice to be ~ 27 Mpa (Arakawa et al. 2000), we consider an icy shell fractured by an impact when $P_d \gtrsim 27$ Mpa.

The icy shell of Enceladus is thought to be ~ 40 km thick globally, thinning to ~ 15 km at the north pole and ~ 9 km at the south pole (Hemingway & Mittal 2019). Adopting these estimates, an icy impactor with radius $R \gtrsim 65$ m is capable of fracturing the south pole, one with $R \gtrsim 110$ m could fracture the north pole, and one with $R \gtrsim 280$ m is able to fracture the icy shell of any other region on Enceladus.

2.2. Fracture rate

The current cratering rate of Enceladus by heliocentric debris with radius $R > 0.75$ km is $3.7 \times 10^{-14} \text{ km}^{-2} \text{ yr}^{-1}$ for Case A¹ and $2.8 \times 10^{-13} \text{ km}^{-2} \text{ yr}^{-1}$ for Case B², each regarded as uncertain to a factor of 4 (Dones et al. 2009). We adopt the following size distribution for impactors, as constrained independently from Kuiper Belt

collisional evolution models and from the crater size distributions of Saturnian moons: $N(> R) \propto R^{1-q}$, where

$$q \sim \begin{cases} 4.0, & R > 30 \text{ km}, \\ 2.0, & 10 \text{ km} < R < 30 \text{ km}, \\ \gamma, & 1 \text{ km} < R < 10 \text{ km}, \\ 2.6, & 0.1 \text{ km} < R < 1 \text{ km}, \\ 3.7, & R < 0.1 \text{ km}, \end{cases} \quad (2)$$

and where we consider the cases of $\gamma = 5.8$ (Minton et al. 2012) and of $\gamma = 4.2$ (Schlichting et al. 2013). We note that there exists uncertainty of the extrapolation below the quoted lower limit of $R \sim 10$ m (Minton et al. 2012; Schlichting et al. 2013).

We use the cumulative size distribution of impactors, combined with our fracture model, to compute the fracture timescale as a function of shell thickness for a pole on Enceladus, as shown in Figure 1. Only the ‘lunar-like’ SPT age of ~ 1 Myr derived by Cassini is compatible with the impactor rates, and itself is more compatible with Case B than Case A, with a best-fit of ‘ $2 \times$ Case B’. $2 \times$ Case B implies a fracture timescale of $\sim 10^6$ yr for the south pole, $\sim 5 \times 10^6$ yr for the north pole, and $\sim 3 \times 10^6$ yr for the remainder of Enceladus. These results suggest that over 1 Gyr, $\sim 10^3$ fractures form on Enceladus, with the majority occurring on the South Pole, and an enhanced fraction ($\gtrsim 10 \times$) relative to the rest of Enceladus occurring on the North Pole. Once a single fracture is formed, it has been demonstrated that parallel fractures can be formed on short ($\lesssim 1$ Myr) timescales (Hemingway et al. 2019).

3. FRACTURE LIFETIME

3.1. Fracture healing due to mass loss

The Enceladus plumes are estimated to eject H_2O at a rate of $\sim 200 \text{ kg s}^{-1}$ (Hansen et al. 2011). Given that the ‘tiger stripes’ are each separated by ~ 35 km, lateral compression of each fracture due to mass loss occurs at rate of $\sim 1 \text{ m Myr}^{-1}$, and is therefore capable of healing a ~ 1 m fracture in the SPT over ~ 1 Myr. The approximate healing timescale as a function of fracture width is indicated in Figure 2. The nozzles located within the ‘tiger stripes’ from which mass is ejected have been estimated to have widths of ~ 0.1 m or of ~ 1 m (Schmidt et al. 2008; Yeoh et al. 2015). Nozzles with widths ~ 1 m (Yeoh et al. 2015) would be completely consistent with the fact that the plumes from the south pole are still observed today and that they are currently unique on Enceladus’ surface.

¹ Consistent with the distribution of small comets at Jupiter and its satellites, and requiring planetocentric debris at Saturn.

² Consistent with the distribution of small craters on Triton, and not necessarily requiring planetocentric debris.

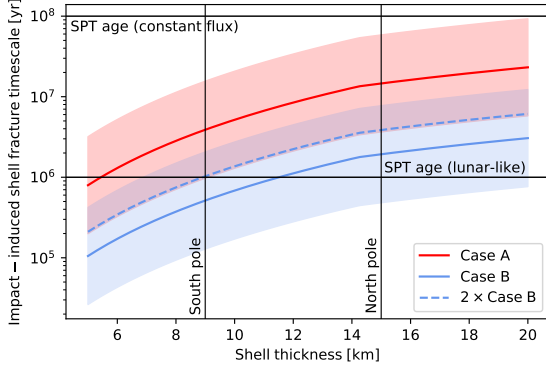


Figure 1. Timescale of impact-induced shell fracture as a function of shell thickness for a pole (constituting ~ 0.1 of the total surface area) on Enceladus. No significant differences exist between $\gamma = 4.2$ and $\gamma = 5.8$. The remainder of Enceladus’ surface (covered by a ~ 40 km shell) would fracture on a timescale of $\sim 3 \times 10^6$ yr for $2 \times$ Case B (the best fit for the Cassini-measured age of the SPT).

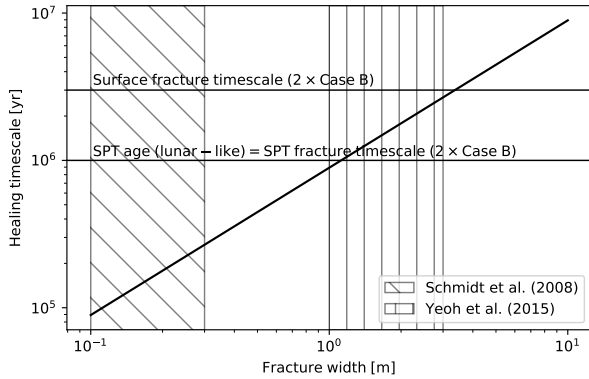


Figure 2. Healing timescale (in yr) as a function of fracture width (in m) due to mass loss from fractures, taken to be $\sim 200 \text{ kg s}^{-1}$. The distance scale on which the resulting compression can heal a fracture of a given width is taken to be the distance between the ‘tiger stripes’, ~ 35 km.

3.2. Impact Resurfacing

We propose that small impactors, which melt surface ice upon impact, could seal off these nozzles and arrest the lifetimes of any resulting plumes. While the surface pressure of the vents is ~ 1 kPa, thin sheets of ice fail at pressures of $\gtrsim 1$ Mpa (Zhang et al. 2012; Wu & Prakash 2015; Qi et al. 2017), making them effective at sealing off nozzles once formed.

For a $\sim 20 \text{ km s}^{-1}$ impactor into ~ 50 K ice, the total melt mass is $\sim 10^2$ times that of the impactor (Kraus et al. 2011). Following the scaling relations for H_2O ice (Kraus et al. 2011), we find that the concentration of

impact melt in a small plug in the crater floor (Senft & Stewart 2011) has surface area,

$$A \sim 1.3 \times 10^4 \text{ m}^2 \left(\frac{R}{10 \text{ m}} \right)^{7/4} \left(\frac{v}{20 \text{ km s}^{-1}} \right)^{2/3}, \quad (3)$$

and thickness,

$$\tau \sim 1.4 \text{ m} \left(\frac{R}{10 \text{ m}} \right)^{7/4} \left(\frac{v}{20 \text{ km s}^{-1}} \right)^{2/3}. \quad (4)$$

The timescales on which these melt plugs cover the entire surface of Enceladus as a function of impactor diameter considered (using the differential size distribution of impactors extrapolated to the relevant size) are shown for a variety of size distributions in Figure 3, with the SPT age and the $2 \times$ Case B surface fracture timescale for reference. The width of the nozzle corresponds directly to the impactor size scale considered, since smaller impactors are more numerous but ones that are smaller than the width of the nozzle could fall inside of it. We would not expect to observe crater morphology on the timescale of a resurfacing since our requirement that melt plugs cover the entire surface dictates that the larger craters must overlap with several others, eroding most resulting topology. Compatible timescales are longer than the SPT age, otherwise we would not currently observe plumes, and shorter than the Case B surface fracture timescale, which would ensure that any trace of old fractures on the surface would be obscured by an ice sheet. These conditions are consistent with all four size distributions considered, but combination of Case B and $\gamma = 5.8$ is disfavored since it would require impactors, and therefore fractures, with widths ~ 10 m.

We also compute the total implied thickness of ice due to resurfacing over 4 Gyr. Enceladus has a deficiency of craters with diameters $\lesssim 2$ km and $\gtrsim 6$ km compared to the other satellites of Saturn. While the low abundance of large craters could be attributed to viscous relaxation, the $\gtrsim 2$ km craters are thought to be filled in by SPT plume material (Kirchoff & Schenk 2009), which could contribute $\sim 2 \times 10^2 - \sim 4 \times 10^2$ m of material over 4 Gyr (Tian et al. 2007). We use the crater depth-diameter relationship as observed on Galilean icy satellites to estimate the depth of a $D \sim 2$ km crater to be ~ 400 m (Schenk 2002). In order to match the observed dearth of $\gtrsim 2$ km craters, impactor resurfacing could have contributed $\lesssim 2 \times 10^2$ m of material, as indicated in Figure 4. This condition is consistent with all four size distributions considered, although it disfavors the combination of Case B and $\gamma = 5.8$.

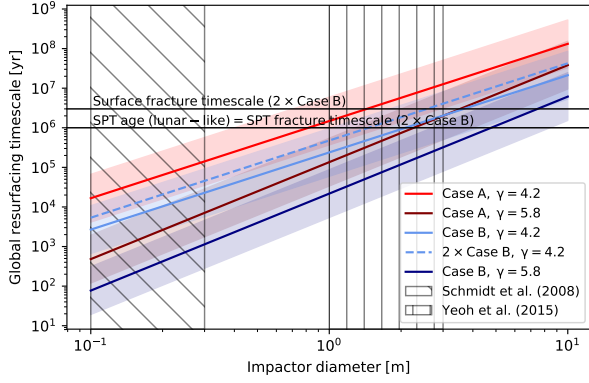


Figure 3. Global resurfacing timescale as a function of impactor diameter.

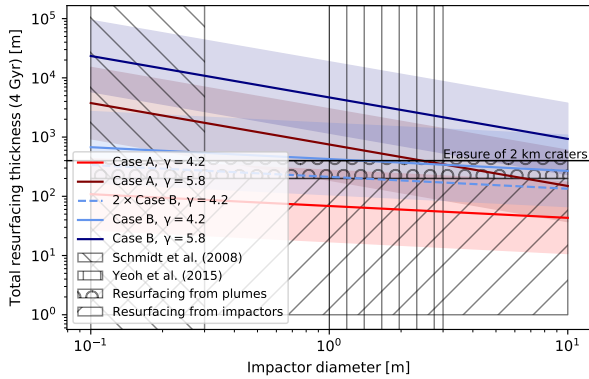


Figure 4. Total resurfacing thickness from impacts over 4 Gyr as a function of impactor diameter.

4. DISCUSSION

Our model of repeatedly generated plumes on Enceladus predicts $\sim 10^3$ independent plume systems per Gyr, the vast majority originating from the South pole with the rest originating elsewhere on the surface, including an enhanced occurrence density at the north pole due to its relatively thin ice. Our model is dependent

on ice thickness. As models of the current state as well as the evolution of Enceladus' icy shell improve, our model's predictions will become more precise.

Our model is consistent with the age of the SPT derived from Cassini data for a lunar-like bombardment history, and inconsistent with a constant flux, making the existence of an early bombardment an important test for our model (Porco et al. 2006). As a result, Case B is strongly favored over Case A, implying that the bombardment history on Enceladus is similar to that of Triton (Dones et al. 2009).

We consider the size distributions presented by Minton et al. (2012) and Schlichting et al. (2013), which differ significantly on the differential size distribution index for radii between 1 km and 10 km, the former predicting $\gamma = 5.8$ and the latter predicting $\gamma = 4.2$. Our model disfavors the combination of Case B and $\gamma = 5.8$ because the implied level of impact resurfacing over 4 Gyr would erase craters larger than ~ 2 km in size, which would be inconsistent with observations (Kirchoff & Schenk 2009), and the nozzle widths would have to be ~ 10 m to be consistent with observations, a value which is larger than predicted (Yeoh et al. 2015). Our model favors $\gamma = 4.2$, and nozzle widths of order 1 m (Yeoh et al. 2015) over nozzle widths of order 0.1 m (Schmidt et al. 2008).

Without fine-tuning, this model for impact-driven plume formation over Myr timescales is consistent with all observations, indicating its strength. Future constraints on the size distribution of small impactors on Enceladus will inform the model parameters. But already now, our model is compatible with the wide range of surface ages and features observed on Enceladus (Porco et al. 2006; Patthoff & Kattenhorn 2011), as well as the predictions made by Hemingway et al. (2019) relating to the younger ages of the non-central fractures in the SPT.

ACKNOWLEDGEMENTS

This work was supported in part by a grant from the Breakthrough Prize Foundation.

REFERENCES

- Arakawa, M., Shirai, K., & Kato, M. 2000, *Geophys. Res. Lett.*, 27, 305
- Benner, S. A. 2017, *Astrobiology*, 17, 840
- Craft, K., Sekhar, P., King, S. D., & Lowell, R. P. 2011, in *AGU Fall Meeting Abstracts*, Vol. 2011, P11B-1596
- Czechowski, L. 2014, *Planet. Space Sci.*, 104, 185
- Dones, L., Chapman, C. R., McKinnon, W. B., et al. 2009, *Icy Satellites of Saturn: Impact Cratering and Age Determination*, ed. M. K. Dougherty, L. W. Esposito, & S. M. Krimigis, 613
- Glein, C. R., & Waite, J. H. 2020, *Geophys. Res. Lett.*, 47, e85885
- Hansen, C. J., Shemansky, D. E., Esposito, L. W., et al. 2011, *Geophys. Res. Lett.*, 38, L11202

- Hemingway, D. J., & Mittal, T. 2019, *Icarus*, 332, 111
- Hemingway, D. J., Rudolph, M. L., & Manga, M. 2019, *Nature Astronomy*, 4
- Hsu, H.-W., Postberg, F., Sekine, Y., et al. 2015, *Nature*, 519, 207
- Hurford, T. A., Bills, B. G., Helfenstein, P., et al. 2009, *Icarus*, 203, 541
- Ingersoll, A. P., & Nakajima, M. 2016, *Icarus*, 272, 319
- Judge, P. 2017, *Astrobiology*, 17, 852
- Kirchoff, M. R., & Schenk, P. 2009, *Icarus*, 202, 656
- Kite, E. S., & Rubin, A. M. 2016, *Proceedings of the National Academy of Science*, 113, 3972
- Klenner, F., Postberg, F., Hillier, J., et al. 2020, *Astrobiology*, 20, 179
- Kraus, R. G., Senft, L. E., & Stewart, S. T. 2011, *Icarus*, 214, 724
- Le Gall, A., Leyrat, C., Janssen, M. A., et al. 2017, *Nature Astronomy*, 1, 0063
- Manga, M., & Wang, C. Y. 2007, *Geophys. Res. Lett.*, 34, L07202
- McKay, C. P., Davila, A., Glein, C. R., Hand, K. P., & Stockton, A. 2018, *Enceladus Astrobiology, Habitability, and the Origin of Life*, ed. P. M. Schenk, R. N. Clark, C. J. A. Howett, A. J. Verbiscer, & J. H. Waite, 437
- Minton, D. A., Richardson, J. E., Thomas, P., Kirchoff, M., & Schwamb, M. E. 2012, in *Asteroids, Comets, Meteors 2012*, Vol. 1667, 6348
- Nimmo, F., & Pappalardo, R. T. 2006, *Nature*, 441, 614
- Patthoff, D. A., & Kattenhorn, S. A. 2011, *Geophys. Res. Lett.*, 38, L18201
- Porco, C., DiNino, D., & Nimmo, F. 2014, *AJ*, 148, 45
- Porco, C. C., Helfenstein, P., Thomas, P. C., et al. 2006, *Science*, 311, 1393
- Postberg, F., Khawaja, N. A., Kempf, S., et al. 2017, in *Lunar and Planetary Science Conference, Lunar and Planetary Science Conference*, 1401
- Qi, C., Lian, J., Ouyang, Q., & Zhao, X. 2017, *Latin American Journal of Solids and Structures*, 14, 1669 . http://www.scielo.br/scielo.php?script=sci_arttext&pid=S1679-78252017000901669&nrm=iso
- Roberts, J. H., & Stickle, A. M. 2017, in *Lunar and Planetary Science Conference, Lunar and Planetary Science Conference*, 1955
- Rudolph, M. L., & Manga, M. 2009, *Icarus*, 199, 536
- Schenk, P. M. 2002, *Nature*, 417, 419
- Schlichting, H. E., Fuentes, C. I., & Trilling, D. E. 2013, *AJ*, 146, 36
- Schmidt, J., Brilliantov, N., Spahn, F., & Kempf, S. 2008, *Nature*, 451, 685
- Senft, L. E., & Stewart, S. T. 2011, *Icarus*, 214, 67
- Shirai, K., Kato, M., Mitani, N. K., & Arakawa, M. 2008, *Journal of Geophysical Research (Planets)*, 113, E11002
- Tajeddine, R., Soderlund, K. M., Thomas, P. C., et al. 2017, *Icarus*, 295, 46
- Taubner, R.-S., Olsson-Francis, K., Vance, S. D., et al. 2020, *SSRv*, 216, 9
- Thomas, P. C., Tajeddine, R., Tiscareno, M. S., et al. 2016, *Icarus*, 264, 37
- Tian, F., Stewart, A. I. F., Toon, O. B., Larsen, K. W., & Esposito, L. W. 2007, *Icarus*, 188, 154
- Travis, B. J., & Schubert, G. 2015, *Icarus*, 250, 32
- Waite, J. H., Glein, C. R., Perryman, R. S., et al. 2017, *Science*, 356, 155
- Wu, X., & Prakash, V. 2015, *International Journal of Impact Engineering*, 76, 155 . <http://www.sciencedirect.com/science/article/pii/S0734743X14002322>
- Yeoh, S. K., Chapman, T. A., Goldstein, D. B., Varghese, P. L., & Trafton, L. M. 2015, *Icarus*, 253, 205
- Zhang, L., Li, Z., Jia, Q., & Huang, W. 2012, *Transactions of Tianjin University*, 18, 112. <https://doi.org/10.1007/s12209-012-1631-y>